Centrum voor Wiskunde en Informatica

CORE

Metadata, citation and similar papers at core.ac.uk

REPORT*RAPPORT*

MAS

Modelling, Analysis and Simulation

Modelling, Analysis and Simulation

Diffusion correction to the avalanche-to-streamer transition

C. Montijn, U. Ebert

REPORT MAS-E0515 AUGUST 2005

CWI is the National Research Institute for Mathematics and Computer Science. It is sponsored by the Netherlands Organization for Scientific Research (NWO).
CWI is a founding member of ERCIM, the European Research Consortium for Informatics and Mathematics.

CWI's research has a theme-oriented structure and is grouped into four clusters. Listed below are the names of the clusters and in parentheses their acronyms.

Probability, Networks and Algorithms (PNA)

Software Engineering (SEN)

Modelling, Analysis and Simulation (MAS)

Information Systems (INS)

Copyright © 2005, Stichting Centrum voor Wiskunde en Informatica
P.O. Box 94079, 1090 GB Amsterdam (NL)
Kruislaan 413, 1098 SJ Amsterdam (NL)
Telephone +31 20 592 9333
Telefax +31 20 592 4199

ISSN 1386-3703

Diffusion correction to the avalanche-to-streamer transition

ABSTRACT
Space-charge dominated streamer discharges can emerge in free space from single electrons if the electric field exceeds a threshold value. We show that this threshold field depends not only on ionization and attachment rates and gap length as suggested by Meek's criterion, but also on electron diffusion. We present analytical and numerical results and derive explicit criteria for streamer formation after the emergence of the first free electron.

2000 Mathematics Subject Classification: 82D10
Keywords and Phrases: Electron avalanche; negative streamers ; minimal streamer model; diffusion.
Note: Financial support for C. Montijn is provided by NWO in the Computational Science program.

Diffusion correction to the avalanche–to–streamer transition

Carolynne Montijn[1], Ute Ebert[1,2]
[1] *CWI, P.O.Box 94079, 1090 GB Amsterdam, The Netherlands, and*
[2] *Dept. Physics, Eindhoven Univ. Techn., The Netherlands.*
(Dated: August 6, 2005)

Space-charge dominated streamer discharges can emerge in free space from single electrons if the electric field exceeds a threshold value. We show that this threshold field depends not only on ionization and attachment rates and gap length as suggested by Meek's criterion, but also on electron diffusion. We present analytical and numerical results and derive explicit criteria for streamer formation after the emergence of the first free electron.

PACS numbers: 52.80.-s,51.50.+v,52.27.Aj,52.27.Cm

I. PROBLEM SETTING AND REVIEW

We investigate the conditions under which a tiny ionization seed in a homogeneous electric field grows out into a streamer with self-induced space charge effects and consecutive rapid growth. Streamers in turn play a role in creating the paths of sparks and lightning [1, 2], in high altitude sprite discharges above thunderclouds [3–5]. They are also used for various industrial applications [6], e.g. corona reactors for water and gas treatment [7–10], and sources of excimer radiation for material processing [11–13]

In narrow geometries, streamers frequently are growing from pointed electrodes, that create strong local fields in their neighborhood. At the electrodes, surface effects take place, and both positive and negative streamers can emerge [14]. On the other hand, in many natural discharges and, in particular, for sprites above thunderclouds [5], it is appropriate to assume that the electric field is homogeneous and boundary effects do not play a role. Of course, dust particles or other nucleation centers can play an additional role in discharge generation, but in the present paper we will focus on the effect of a homogeneous field on a homogeneous gas. This assumption corresponds to the case discussed previously, e.g., in [15–17] and will be subject of the present paper.

Typically, the avalanche to streamer transition is assumed to depend on the ionization rate α and gap length d through the dimensionless combination αd. We here first recall this statement and then reinvestigate the problem and find, that the transition depends also on electron diffusion. This dependence is analyzed quantitatively in full parameter space.

In detail, we consider a continuous discharge model with attachment and local field-dependent impact ionization rate and space charge effects. It is defined through

$$\begin{aligned}
\partial_t n_e &= D_e \nabla^2_{\mathbf{R}} n_e + \nabla_{\mathbf{R}} \cdot (\mu_e \mathbf{E}\, n_e) \\
&\quad + (\mu_e |\mathbf{E}|\, \alpha(|\mathbf{E}|) - \nu_a)\, n_e, \\
\partial_t n_+ &= \mu_e \mathbf{E}\, \alpha(|\mathbf{E}|)\, n_e, \\
\partial_t n_- &= \nu_a\, n_e, \\
\nabla^2_{\mathbf{R}} \Phi &= \frac{\mathrm{e}}{\epsilon_0}\,(n_e + n_- - n_+) \quad , \quad \mathbf{E} = -\nabla_{\mathbf{R}} \Phi. \qquad (1)
\end{aligned}$$

Here n_e, n_+ and n_- are the particle densities of electrons, positive and negative ions, and $\mathbf{E}$ and Φ are the electric field and potential, respectively. D_e and ν_a are the electron diffusion coefficient and the electron attachment rate. We assume the impact ionization rate $\alpha(\mathbf{E})$ to be a function of the electric field, and for our numerical calculations, we use the Townsend approximation $\alpha(|\mathbf{E}|) = \alpha_0 \exp(-E_0/|\mathbf{E}|)$, in which α_0 and E_0 are parameters for the effective cross section. The positive and negative ions are considered to be immobile on the time scales investigated in this paper. The initial ionization seed is placed in free space, and an electron avalanche drifts towards the anode.

Eventually, the charged particle density in the avalanche will grow so large that space charge effects set in and change the externally applied field, and a streamer emerges from the avalanche. Essentially two criteria have been given in the literature for this emergence of a streamer from a tiny ionization seed. The first one is a necessary lower bound: the electric field has to be higher than the threshold field E_k where the impact ionization rate overcomes the attachment rate. Only for $|\mathbf{E}| > E_k$, the ionization level can grow. Here E_k is defined through

$$\mu_e\, E_k\, \alpha(E_k) = \nu_a. \qquad (2)$$

The second criterion is known as Meek's criterion. As derived originally in [15], it states that for a cathode directed (i.e., positive) streamer to emerge from an anode directed avalanche, the system has to be long enough to allow for a sufficient multiplication of the drifting electron package. Then the electric field of the ions is high enough for secondary emitted electrons at the anode to drift towards the cathode. Typically, multiplication rates by 8 [15, 18] to 9 [17] decades are assumed to be sufficient. This fixes the second criterion as

$$\exp\left[\left(\alpha(|\mathbf{E}|) - \frac{\nu_a}{\mu_e |\mathbf{E}|}\right) d\right] \approx 10^8 \text{ to } 10^9, \qquad (3)$$

where d is the avalanche length. In brief as a rule of thumb the criterion reads

$$\alpha(|\mathbf{E}|)\, d \approx 18 \text{ to } 21 \quad \text{according to Meek.} \qquad (4)$$

Meek's criterion has been extended to the transition of the avalanche to an anode directed (i.e., negative) streamer [16, 17].

In the present paper we argue that for an avalanche originating from a tiny local seed, this criterion is not sufficient since it neglects the diffusion of the electron package. Diffusion decreases the electron density while impact ionization increases it. In low fields, diffusion stays dominant for all times which will always suppress space charge effects and consecutive streamer emergence.

The difference is particularly pronounced in non-attaching gases like nitrogen. Here Meek's criterion would suggest that streamer formation could take place as long as there is any impact ionization and the system is sufficiently long. However, electron diffusion will suppress streamer formation in low fields.

We will elaborate this argument analytically and numerically, and we will give quantitative corrections to the above criteria. First the intrinsic scales of the problem with their explicit density dependence are identified through dimensional analysis. Then analytical results for the electron density are recalled and the electron induced field is calculated. This gives a lower bound for the time and travel distance of avalanche-to-streamer transition. The ion density distribution cannot be calculated analytically, however, we found that all spatial moments of the distribution can be calculated. These moments provide the basis for an estimate of the avalanche-to-streamer transition. Fig. 4 summarizes how travel time and distance at the transition depend on applied field and diffusion constant.

II. DIMENSIONAL ANALYSIS

Meek's criterion can be understood as an example of dimensional analysis: the effective cross-section $\alpha(|\mathbf{E}|)$ has the dimension of inverse length, hence $\alpha(|\mathbf{E}|)d$ is a dimensionless number that characterizes a certain behavior. It is useful to extract the intrinsic scales also from other quantities. In particular, there is another dimensionless number in the problem, namely the dimensionless diffusion constant

$$D = \frac{D_e \alpha_0}{\mu_e E_0}, \tag{5}$$

that plays a distinctive role in the avalanche to streamer transition as well. Note that this dimensionless diffusion constant in general depends on temperature as D_e/μ_e seems to be well approximated by the Einstein relation $D_e/\mu_e = kT/e$ where k is Boltzmann's constant and T the temperature [16].

In general, lengths are measured in units of $1/\alpha_0$, fields in units of E_0, and velocities in units of $\mu_0 E_0$ as in [19] — hence diffusion should be measured in units of $\mu_e E_0/\alpha_0$ as done in (5). The parameters α_0, μ_e, D_e and E_0 depend on density, and for N_2 they are [16, 20–22]:

$$\alpha_0^{-1} = 2.3\ \mu\mathrm{m}\ \frac{1}{N/N_0}, \qquad E_0 = 200\ \frac{\mathrm{kV}}{\mathrm{cm}}\ \frac{N}{N_0}, \tag{6}$$

$$\mu_e = 380\ \frac{\mathrm{cm}^2}{\mathrm{Vs}}\ \frac{1}{N/N_0}, \qquad D_e = 1800\ \frac{\mathrm{cm}^2}{\mathrm{s}}\ \frac{1}{N/N_0}, \tag{7}$$

where N_0 is the normal atmospheric particle density. At room temperature, the dimensionless diffusion coefficient with these parameters becomes $D \approx 0.1$.

Dimensionless parameters and fields are introduced as

$$\mathbf{r} = \alpha_0\, \mathbf{R}, \qquad \tau = \alpha_0 \mu_e E_0\, t,$$
$$\sigma = \frac{\mathrm{e}\, n_e}{\epsilon_0 \alpha_0 E_0}, \qquad \rho = \frac{\mathrm{e}\,(n_+ - n_-)}{\epsilon_0 \alpha_0 E_0},$$
$$\boldsymbol{\mathcal{E}} = \frac{\mathbf{E}}{E_0}, \qquad \nu = \frac{\nu_a}{\alpha_0 \mu_e E_0},$$

which brings the system of equations (1) into the dimensionless form

$$\partial_\tau\, \sigma = D\nabla^2\sigma + \nabla(\boldsymbol{\mathcal{E}}\sigma) + f(|\boldsymbol{\mathcal{E}}|,\nu)\,\sigma\,, \tag{8}$$
$$\partial_\tau\, \rho = f(|\boldsymbol{\mathcal{E}}|,\nu)\,\sigma\,, \tag{9}$$
$$\nabla^2\phi = -\nabla\cdot\boldsymbol{\mathcal{E}} = \sigma - \rho\,, \tag{10}$$

where

$$f(|\boldsymbol{\mathcal{E}}|,\nu) = |\boldsymbol{\mathcal{E}}| e^{-1/|\boldsymbol{\mathcal{E}}|} - \nu, \tag{11}$$

and the operator ∇ is taken with respect to $\mathbf{r}$. The advantage of using these dimensionless quantities is the scaling with number density, which makes the translation of the results to any pressure straightforward.

It is remarkable that the density of positive and negative ions $n_\pm$ enters the equations only in the form of the single dimensionless field $\rho \propto n_+ - n_-$. This is clear in the case of the Poisson equation, but holds also for the generation term proportional to $f(|\boldsymbol{\mathcal{E}}|,\nu)$.

We neglect the effect of photoionization as it is an induced effect of impact ionization. Therefore photoionization rates are typically much lower than impact ionization rates and do not contribute significantly to the build-up of a compact ionization seed that is required for an avalanche to streamer transition.

An initial ionization seed will under influence of the background electric field advect towards the anode, diffuse and grow due to ionizing collisions with neutral atoms. At the beginning of this process the influence of space charges on the electric field is negligible. We can therefore analyze the continuity equations Eqs. (8)-(9) in a homogeneous background field $\boldsymbol{\mathcal{E}}_b$, which makes the process linear. Eventually space charges do affect the electric field, and the streamer regime is reached. Then charged layers emerge, shielding the interior of the streamer from the outer electric field. We here investigate when this will happen.

III. ELECTRON DISTRIBUTION AND FIELD

A. Exact result for the electron distribution

We write the single electron that generates the avalanche as a localized initial density

$$\sigma(\mathbf{r}, \tau = 0) = \rho(\mathbf{r}, \tau = 0) = \sigma_0 \delta(\mathbf{r} - \mathbf{r_0}) \qquad (12)$$

and consider its evolution, in a cylindrically symmetric coordinate system, under influence of a uniform field $\boldsymbol{\mathcal{E}}_b = -\mathcal{E}_b \hat{\mathbf{e}}_z$, $\hat{\mathbf{e}}_z$ being the unit vector along the axial direction.

To approximate the single electron, one has to take $\sigma_0 = 10^{-4}$ at atmospheric pressure. Indeed the integration over the whole space of the initial electron density distribution (12) is, obviously, equal to σ_0. Using the dimensional analysis introduced in previous section, this corresponds to a total number of $(\sigma_0 n_0)/\alpha_0^3$ electrons, which is assumed to be unity (n_0 being the characteristic particle density, $n_0 = \epsilon_0 \alpha_0 E_0/e$). A substitution of the numerical values for the intrinsic scales then leads to $\sigma_0 = 10^{-4}/(N/N_0)$. For this initial condition, the electron evolution according to Eq. (8) can be given explicitly as [16]

$$\sigma(\mathbf{r}, \tau) = \sigma_0 \, e^{f\tau} \, \frac{e^{-(\mathbf{r}-\mathbf{r}_0-\boldsymbol{\mathcal{E}}_b\tau)^2/(4D\tau)}}{(4\pi D\tau)^{3/2}}; \qquad (13)$$

it has the form of a Gaussian package that drifts with velocity $-\boldsymbol{\mathcal{E}}_b$, widens diffusively with half width proportional to $\sqrt{4D\tau}$, and carries a total number of electrons $e^{f\tau}$. (If the initial ionization seed consists of several electrons in some close neighborhood, the Gaussian shape is approached nevertheless for large times due to the central limit theorem.)

It should be noted that while the total number of electrons in the package grows exponentially in time, the maximum of the electron density

$$\sigma_{\max}(\tau) = \max_{\mathbf{r}} \sigma(\mathbf{r}, \tau) = \frac{\sigma_0 \, e^{f\tau}}{(4\pi D\tau)^{3/2}} \qquad (14)$$

first decreases until $\tau = 3/(2f)$ and then increases. At this moment of evolution, generation overcomes diffusion.

B. Exact result for the electron generated field $\mathcal{E}_\sigma$

While density and field of the ions can only be calculated approximately and will be treated in the next section, the electric field $\boldsymbol{\mathcal{E}}_\sigma$ generated by the Gaussian electron package can be calculated exactly. The main point is that the electron density distribution (13) is spherically symmetric about the point $\mathbf{r}_0 + \boldsymbol{\mathcal{E}}_b\tau$. The electric field $\boldsymbol{\mathcal{E}}_\sigma(s, \tau)$ induced by the electrons at the point $\mathbf{s} = \mathbf{r} - \mathbf{r}_0 - \boldsymbol{\mathcal{E}}_b\tau$ can therefore be written as $\boldsymbol{\mathcal{E}}_\sigma = -\mathcal{E}_\sigma \hat{\mathbf{e}}_s$, where $\hat{\mathbf{e}}_s$ is the unit vector in the radial $\mathbf{s}$ direction. Its magnitude can be computed with Gauss' law of electrostatics:

$$\begin{aligned} \mathcal{E}_\sigma(s, \tau) &= -\frac{1}{s^2} \int_0^s \sigma_0 e^{f\tau} \, \frac{e^{-r^2/(4D\tau)}}{(4\pi D\tau)^{3/2}} \, r^2 dr \\ &= -\frac{\sigma_0 e^{f\tau}}{16\pi D\tau} \, F\left(\frac{s}{\sqrt{4D\tau}}\right), \end{aligned} \qquad (15)$$

with

$$F(x) = \frac{1}{x^2} \, \frac{4}{\sqrt{\pi}} \int_0^x y^2 e^{-y^2} dy = \frac{\mathrm{erf}\, x}{x^2} - \frac{2}{\sqrt{\pi}} \, \frac{e^{-x^2}}{x}, \qquad (16)$$

where erf is the error function. The spatial maximum of the field $\mathcal{E}_\sigma$ is determined by the maximum of $F(x)$; it is given by

$$\frac{2}{\sqrt{\pi}}(x + x^3)e^{-x^2} = \mathrm{erf}\; x. \qquad (17)$$

Solving this equation numerically leads to a position of the maximum of about $x \simeq 1$ and to the value $F(1) \simeq 0.4276$. The spatial maximum of the electron generated electric field becomes

$$\mathcal{E}_\sigma^{max}(\tau) \simeq \frac{\sigma_0 e^{f\tau}}{16\pi D\tau} F(1), \qquad (18)$$

it is located on the sphere parameterized through

$$|\mathbf{r} - \mathbf{r}_0 - \boldsymbol{\mathcal{E}}_b\tau| \simeq \sqrt{4D\tau}. \qquad (19)$$

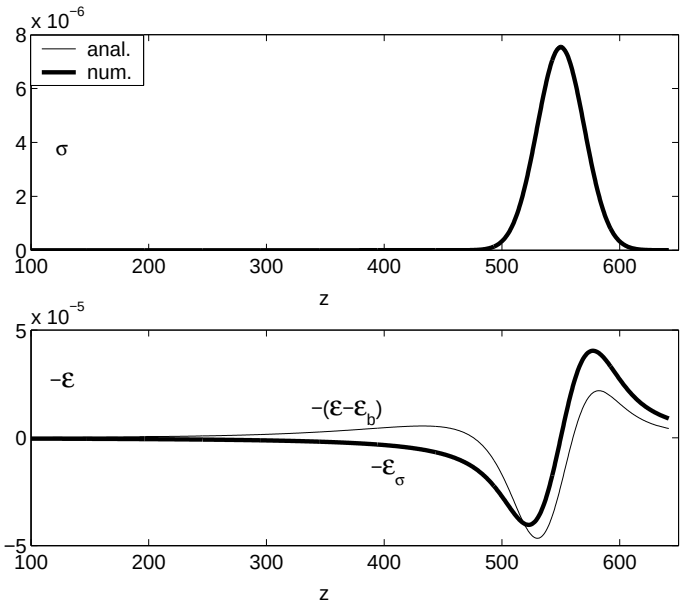

FIG. 1: Numerical and analytical results at $\tau = 2000$ on the axis of symmetry z when the externally applied field is $\boldsymbol{\mathcal{E}}_b = -0.25 \, \hat{\mathbf{e}}_z$, and $D = 0.1$, $\nu = 0$ and $\sigma_0 = 10^{-4}$. The initial condition is located at $\mathbf{r}_0 = 50 \, \hat{\mathbf{e}}_z$. The upper figure shows the electron density; the analytical expression coincides with the numerical result as it should. The lower figure shows the axial component (pointing in the same direction as $\boldsymbol{\mathcal{E}}_b$) of the numerically computed field strength $\boldsymbol{\mathcal{E}} - \boldsymbol{\mathcal{E}}_b$ due to both electrons and ions (thick line) and the analytical result for the field $\boldsymbol{\mathcal{E}}_\sigma$ induced by the electrons only (thin line).

C. A lower bound for the transition

The electric field generated by the electrons leads to a first estimate for the avalanche to streamer transition. Actually, the magnitude of the monopole field $\mathcal{E}_\sigma$ ahead of the electron cloud is an upper bound for the magnitude of the field created by the dipole of electrons on the one hand and the positive charges left behind by the electron cloud on the other hand (see lower panel in Fig. 1). Therefore, substantial fields arise after a shorter travel time τ_0 and distance, so that τ_0 is a lower bound for the time $\tau_{a\to s}$ of the avalanche-to-streamer transition.

The space charge generated field is measured relative to the externally applied field E_b as $|E^{max}(\tau) - E_b| \leq k|E_b|$. We will show in the next section that $k = 0.03$ is an appropriate estimate for the mid gap avalanche to streamer transition.

Finally, the lower bound τ_σ for the transition can be expressed through Eq. (18) as

$$f\tau_\sigma - \ln(\mathcal{E}_b\tau_\sigma) \simeq \ln\frac{16\pi kD}{F(1)\sigma_0}. \tag{20}$$

As travel time and travel distance are related through the drift velocity $\mathcal{E}_b$ and working the way back through dimensional analysis, $f(|\boldsymbol{\mathcal{E}}_b|,\nu)\tau_\sigma$ is found to be identical to $(\alpha(|\mathbf{E}_b|) - \nu_a/\mu_e E_b)d_\sigma$, where $d_\sigma = \mu_e E_b t_\sigma$ is the avalanche travel distance. In dimensional quantities, Eq. (20) takes the form

$$\left(\alpha(|E_b|) - \frac{\nu_a}{\mu_e E_b}\right) d_\sigma - \ln(d_\sigma\alpha_0) = \ln\frac{16\pi k10^4}{F(1)} + \ln\frac{D_e\alpha_0}{\mu_e E_0} - \ln\frac{N}{N_0}. \tag{21}$$

For a non-attaching gas ($\nu_a = 0$) at atmospheric pressure under normal conditions with dimensionless diffusion comparable to nitrogen, inserting the numerical values for the parameters, we obtain

$$\alpha(|E_b|)d_\sigma - \ln(\alpha_0 d_\sigma) \approx 9.43. \tag{22}$$

f being a growing function of $|\boldsymbol{\mathcal{E}}_b|$, Eq. (37) shows that the larger the field, the earlier the transition takes place, which is in accordance with Meek's criterion. On the other hand, the second term of in the right hand side of Eq. (21) is dependent on the diffusion coefficient in such a way that diffusion delays the transition to streamer, as expected.

The solution $\alpha(|E_b|)d_\sigma$ for N_2 at atmospheric pressure is shown in the dash-dotted line of Fig. 3, where it is compared to a numerical evaluation of the transition time (symbols). The latter have been obtained through a full simulation of the continuity equations (8)-(9) together with the Poisson equation (10) [23, 24]. Though the qualitative features of the transition time are well reproduced, this figure shows that the underestimation of the transition time is significant, and that it is necessary to include the field of the ion trail left behind by the electrons.

IV. ION DISTRIBUTION AND FIELD

A. Exact results on the spatial moments of the distributions

To get a more accurate estimate for the avalanche-to-streamer transition, the field generated by the positive and negative ions has to be included. In the case of the ion distribution, closed analytical results cannot be found, in contrast to the electron distribution (13). However, arbitrary spatial moments of the distribution

$$\langle\mathcal{O}\rangle_\rho = \frac{\int \mathcal{O}\ \rho\ d^3\mathbf{r}}{\int \rho\ d^3\mathbf{r}}, \quad \text{where} \quad \mathcal{O} = z^n \ \text{ or } \ r^n, \tag{23}$$

can be derived analytically. Here z is the direction of the homogeneous field $\boldsymbol{\mathcal{E}}_b$ and r is the radial direction. First, the evolution equation (9) for the ion density is integrated in time and the analytical form (13) for $\sigma(\mathbf{r},\tau)$ is inserted. As $f = f(|\boldsymbol{\mathcal{E}}_b|,\nu)$ is constant in space and time one finds

$$\rho(\mathbf{r},\tau) - \rho(\mathbf{r},0) = f\sigma_0\int_0^\tau d\tau'\ e^{f\tau'}\ \frac{e^{-(z-z_0-\mathcal{E}_b\tau')^2/(4D\tau')}}{\sqrt{4\pi D\tau'}}\ \frac{e^{-r^2/(4D\tau')}}{4\pi D\tau'}. \tag{24}$$

Here the initial perturbation is located at z_0 on the axis $r = 0$. The moments (23) can now be derived from (24) by exchanging the order of spatial and temporal integration. In particular, one finds

$$\begin{aligned}\int \rho\ d^3\mathbf{r} &= \sigma_0\ e^{f\tau}, \\ \int z\ \rho\ d^3\mathbf{r} &= \sigma_0\ e^{f\tau}\ \left(z_0 + \mathcal{E}_b\tau - \frac{1-e^{-f\tau}}{f/\mathcal{E}_b}\right),\end{aligned} \tag{25}$$

and higher moments can be calculated in the same way. For the moments of ρ, this gives

$$\begin{aligned}\langle z\rangle_\rho &= z_0 + \mathcal{E}_b\left(\tau - \frac{1}{f}\right) + O\left(e^{-f\tau}\right), \\ \langle z^2\rangle_\rho - \langle z\rangle_\rho^2 &= \left(\frac{\mathcal{E}_b}{f}\right)^2 + 2D\left(\tau - \frac{1}{f}\right) + O\left(e^{-f\tau}\right).\end{aligned} \tag{26}$$

The second moment of ρ in the radial direction is

$$\langle r^2\rangle_\rho = 2D\left(\tau - \frac{1}{f}\right) + O\left(e^{-f\tau}\right). \tag{27}$$

For comparison, the moments of the Gaussian electron distribution (13) are easily found to be

$$\langle z\rangle_\sigma = z_0 + \mathcal{E}_b\tau, \tag{28}$$

$$\langle z^2\rangle_\sigma - \langle z\rangle_\sigma^2 = 2D\tau, \tag{29}$$

$$\langle r^2\rangle_\sigma = 2D\tau. \tag{30}$$

B. Discussion of the moments

These moments mean that the center of mass of the electron package is located at $z = z_0 + \mathcal{E}_b\tau$, and the package has a diffusive width $\sqrt{2D\tau}$ around it, both in the forward z direction and in the radial r direction. The second moment in the z direction is calculated relative to the center of mass

$$\langle z^2\rangle_x^c := \left\langle \left(z - \langle z\rangle_x\right)^2 \right\rangle_x = \langle z^2\rangle_x - \langle z\rangle_x^2, \quad x = \sigma, \rho. \tag{31}$$

The ion cloud shows a more complex behavior; it is evaluated close to the avalanche-to-streamer transition where $f\tau = \alpha d = O(10)$, therefore the terms of order $e^{-f\tau}$ are neglected.

First it is remarkable that the center of mass of the ion cloud shifts with precisely the same velocity as the electron cloud though the ion motion is neglected while the electrons drift, and that the ion center of mass is at an approximately constant distance $\mathcal{E}_b/f$ behind the electron center of mass. This distance

$$\ell_\alpha = \frac{\mathcal{E}_b}{f(\mathcal{E}_b)} = \frac{\alpha_0}{\alpha(E_b)} \tag{32}$$

in dimensionless units corresponds to ionization length $1/\alpha(E_b)$.

The square of the radial width of the ion cloud $2D(\tau - 1/f)$ is $2D/f$ smaller than the one of the electron cloud. This is clear since the electron cloud also was more narrow when it left the ions behind. The ion cloud is more extended in the z direction. More precisely, its length is ℓ_α larger than its width. This comes from the ions being immobile, therefore a trace of ions is left behind by the electron cloud. Moreover, it can be remarked that the difference between the width and the length of the ion cloud is the same as the distance between the centers of mass of the ion and the electron cloud, namely the ionization length ℓ_α.

C. An estimate for the transition

One can assume as in [17] that the ions have a distribution similar to the electrons, thus a Gaussian with the same width as the electron cloud, but centered around $(r = 0, z = \langle z\rangle_\rho)$:

$$\rho_1(r, z, \tau) = \sigma_0\, e^{f\tau}\, \frac{e^{-\left[(z-\langle z\rangle_\rho)^2 + r^2\right]/(4D\tau)}}{(4\pi D\tau)^{3/2}}. \tag{33}$$

In this approximation, the total electric field becomes:

$$\boldsymbol{\mathcal{E}}_1(r, z, \tau) = \boldsymbol{\mathcal{E}}_b - \frac{\sigma_0 e^{ft}}{16\pi\, D\tau}\left[F\left(\frac{|\mathbf{s}_\sigma|}{\sqrt{4D\tau}}\right)\frac{\mathbf{s}_\sigma}{|\mathbf{s}_\sigma|} + F\left(\frac{|\mathbf{s}_\rho|}{\sqrt{4D\tau}}\right)\frac{\mathbf{s}_\rho}{|\mathbf{s}_\rho|}\right], \tag{34}$$

where

$$\mathbf{s}_x \;=\; \mathbf{r} - \langle z\rangle_x\, \hat{\mathbf{e}}_z \quad \text{for} \quad x = \rho, \sigma \tag{35}$$

are the distances to the electron and ion centers of mass.

The maximum of the field $\mathcal{E}_1$ can not be computed analytically. However, in Fig. 1 it can be seen that the positions of the maximum of the total field and that of the electron field nearly coincide. Therefore we evaluate the field $\mathcal{E}_1$ at the maximum of $\mathcal{E}_\sigma$ as defined in Eq. (18). Moreover, it is easily seen that the maximum of the field is situated on the axis, ahead of the electron cloud. The maximum of the electric field can thus be approximated as:

$$\begin{aligned}\mathcal{E}_1^{max}(\tau) &\simeq \mathcal{E}_1(r = 0, z = z_0 + \boldsymbol{\mathcal{E}}_b\tau + \sqrt{4D\tau}, \tau)\\ &= \mathcal{E}_b + \frac{\sigma_0 e^{f\tau}}{16\pi D\tau}\left[F(1) - F\left(1 + \sqrt{\frac{\ell_\alpha^2}{4D\tau}}\right)\right].\end{aligned} \tag{36}$$

Then $E_1^{max} - E_b = kE_b$ implies for the transition time τ_1:

$$\begin{aligned}f\tau_1 - \ln(\mathcal{E}_b\tau_1) - \ln\frac{F(1)}{F(1) - F\left(1 + \sqrt{\frac{\ell_\alpha^2}{4D\tau_1}}\right)}\\ = \ln\frac{16\pi kD}{F(1)\sigma_0}\end{aligned} \tag{37}$$

The argument of the logarithm in the third term on the right hand side being larger than 1, this criterion gives a later time for the transition than that based on the field of the electrons only. This is what we expect considering that the ions tend to reduce the field of the electrons, thus the effect of space charge. The correction given by the ion field is a function of the ratio of the ionization length ℓ_α and the diffusion length $\sqrt{2D\tau}$. At early times, this ratio goes to infinity, and the correction given by the ion cloud is negligible. However, at later times, the correction becomes more significant.

Fig. 2 shows the influence of the correction on the field of the electrons, as well as the numerical results for the field of the ion and electron cloud together. It shows that, indeed, the correction only becomes important for larger times.

Moreover, the approximation for the maximal field ahead has now become much better than the previous approximation based on only the electron cloud. Indeed, for e.g the case of $\boldsymbol{\mathcal{E}}_b = 0.5$ (corresponding to the middle thick lines), the numerically computed field (solid line) reaches the transition value ($(\boldsymbol{\mathcal{E}}_{num} - \boldsymbol{\mathcal{E}}_b) = 0.03\boldsymbol{\mathcal{E}}_b$ at $f\tau \approx 14$. When only the field of the electrons is taken into account, this value would already be reached at $f\tau \approx 12.6$, while the correction based on the approximation of the ion cloud leads to a transition time of $f\tau \approx 13.9$. The correction becomes especially important at lower fields. In high fields, the approximation of the ions shows somewhat larger deviations. The figure also shows that the choice of $k = 0.03$ in $E_{max} - E_b = kE_b$ is appropriate for the definition of the transition, since the maximal electron density then drops below the analytical solution with vanishing space charges.

In Fig. 3 we compare the transition times given by Eqs. (20) and (37) with numerically evaluated transition

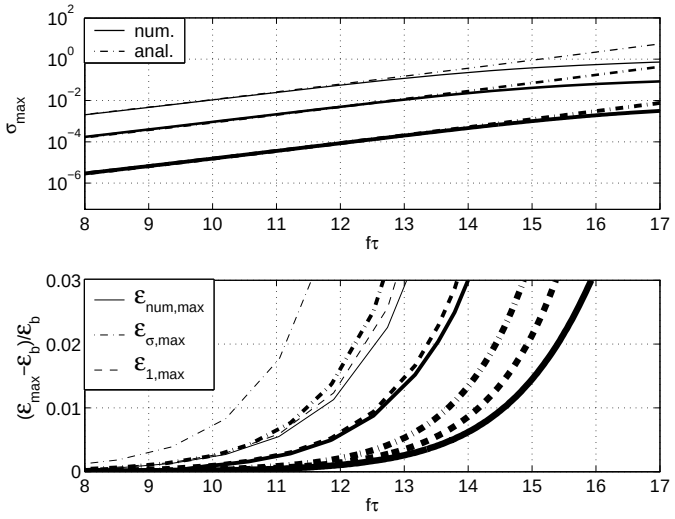

FIG. 2: Evolution of the maximal electron density (upper panel) and electric field (lower panel) as a function of $f\tau$. Different values of $\mathcal{E}_b$ have been chosen: thin line: $\mathcal{E}_b = 1$, 1 line $\mathcal{E}_b = 0.5$ and thick line $\mathcal{E}_b = 0.25$. Upper panel: Numerical results (solid lines) for the maximal electron density compared with Eq. 14 (dash-dotted lines). Lower panel: numerical results (solid lines) are compared to maximum electric field induced by the electrons (dash-dotted lines) on the one hand and the maximal field given by Eq. (36) on the other hand (dashed lines).

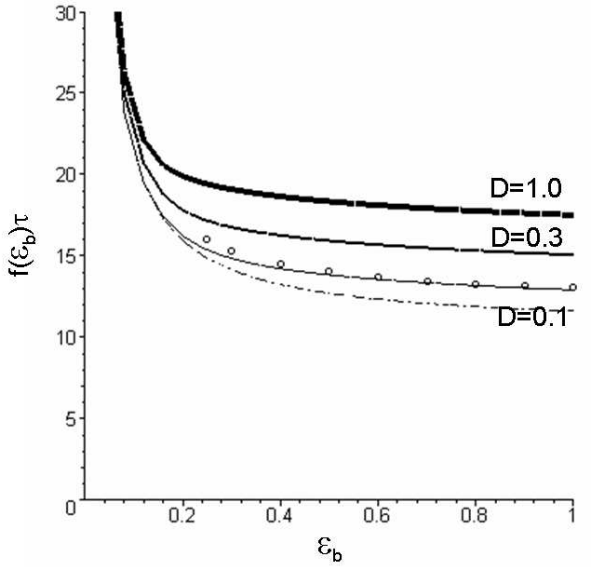

FIG. 3: The transition time $f\tau$ (equivalent to the travel distance αd) as a function of the background electric field for $\sigma_0 = 10^{-4}$, $\nu = 0$ and different values of D. Solid line: computed with Eq. (37) for $D = 0.1$ (thin line), 0.3 (middle thin line) and 1 (thickest line); dash-dotted line: computed with Eq. (20) for $D = 0.1$; symbols: numerical evaluation for $D = 0.1$.

times. It shows that the approximation of similar electron and ion distributions leads to a very good approximation of the transition time. From this figure it is also clear that the transition time $f\tau$ depends strongly on the electric field, and grows larger towards smaller fields. Moreover, looking at the transition time for higher diffusion coefficients, it is seen that diffusion tends to delay the transition to the streamer regime. This can be expected, since diffusion will tend to broaden the electron cloud, thereby suppressing space charge effects.

For completeness, a 3-dimensional plot of the transition time approximated by Eq. (37) as a function of both background electric field and diffusion coefficients is shown in Fig. 4. From this figure, we see that Meek's transition criterion, that stated that $f\tau$ is approximately constant, corresponds to the case of relatively high diffusion and background field. However, realistic values of D are in the range of 0.1 to 0.3 at room temperature, and a background electric field higher than 2 also leads to unrealistic values. So in the parameter range of real experiments, the correction given by Eq.(3) on Meek's criterion can not be neglected.

D. A more accurate approximation for the ion density distribution

The previous approximation ρ_1 of the ion distribution leads to a relatively good approximation for the transition time in the case of a mid-gap transition. However, the real ion distribution is more narrow in the r-direction, and can be wider and asymmetrical in the z-direction. As discussed in [15], it is the field of the ion cloud that should be high to suppress the background field, so that, when the electron cloud has drifted into the anode, new electrons emitted by e.g. photoionization are drawn towards the cathode, creating a positive streamer. In this section we present another approximation for the ion distribution, which will lead to a better overall approximation of the electric field, and of the self field induced by the ion trail. The price however to pay for this is a much more complicated analytical expression for the density and the field.

A better approximation for ρ would be an ellipsoidal Gaussian distribution centered around $(r = 0, z = \langle z\rangle_\rho)$ with width $\langle z^2\rangle_\rho^c = \langle z^2\rangle_\rho - \langle z\rangle_\rho^2$ and $\langle r^2\rangle_\rho^c = \langle r^2\rangle_\rho$ in the z- and r-direction, respectively. The height of this Gaussian should be such that the total amount of ions at time t is still equal to $\sigma_0 e^{ft}$. The appropriate expression for the ion distribution is:

$$\rho(r,z,t) = \frac{\sigma_0 e^{ft}}{(2\pi)^{3/2} S_r^2 S_z} e^{-r^2/(2S_r^2) - (z-\langle z\rangle_\rho)^2/(2S_z^2)} \quad (38)$$

However, as far as we know, no closed analytical expression is known for the field of such an ellipsoidal Gaussian charge distribution. So instead, we take a spherical Gaussian distribution with the same height as the one defined

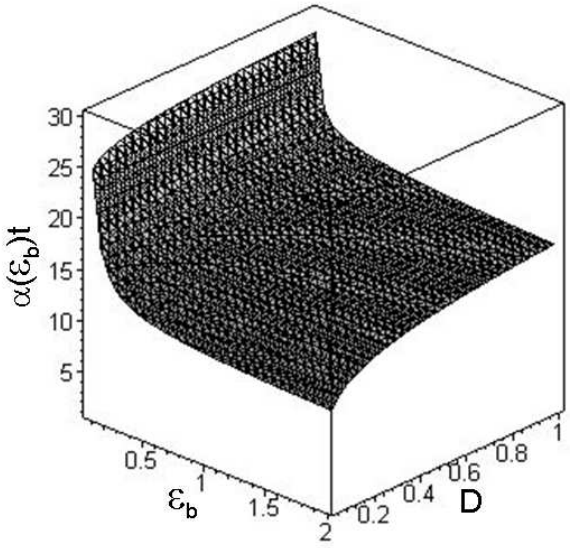

FIG. 4: The transition distance αd according to Eq. 37) as a function of the background electric field $\mathcal{E}_b$ and the diffusion coefficient D for $\sigma_0 = 10^{-4}$ and $\nu = 0$.

in Eq. (38):

$$\rho_2(r,z,\tau) = \frac{\sigma_0 e^{f\tau}}{(2\pi)^{3/2} S_\rho^3} e^{-(r^2+(z-\langle z\rangle_\rho)^2)/(2S_\rho^2)}\,, \qquad (39)$$

where

$$\begin{aligned} S_\rho^3 &= \langle r^2\rangle_\rho^c \sqrt{\langle z^2\rangle_\rho^c} \\ &= \left(2D(\tau-\frac{1}{f})\sqrt{2D(\tau-\frac{1}{f})+l_\alpha^2}\right)\,. \end{aligned} \qquad (40)$$

The electric field induced by this ion distribution is:

$$E_{\rho_2}(r,z,\tau) = \frac{\sigma_0 e^{f\tau}}{8\pi S_\rho^2} F\left(\sqrt{\frac{|\mathbf{s}_\rho|^2}{2S_\rho^2}}\right)\,, \qquad (41)$$

where $\mathbf{s}_\rho$ is defined in Eq. (35).

In Fig. 5 we compare the densities and fields given by the numerical solution and ρ_1 and ρ_2. It shows clearly that the approximation ρ_2 does not give a better approximation of the field ahead of the electron cloud. This can be explained by the fact that, the region ahead of the electron cloud does not contain any ions, so that the field induced by the ions is only a function of the total number of ions, which is the same in both ρ_1 and ρ_2. On the other hand, inside the ion cloud the approximation is much better. Therefore, evaluating the electron and ion densities with Eqs. (13) and (39) and their fields with Eqs. (15) and (41), at the transition time T_1 given by Eq. (37), will give a good approximation of the status of the process at the time that streamer regime is entered.

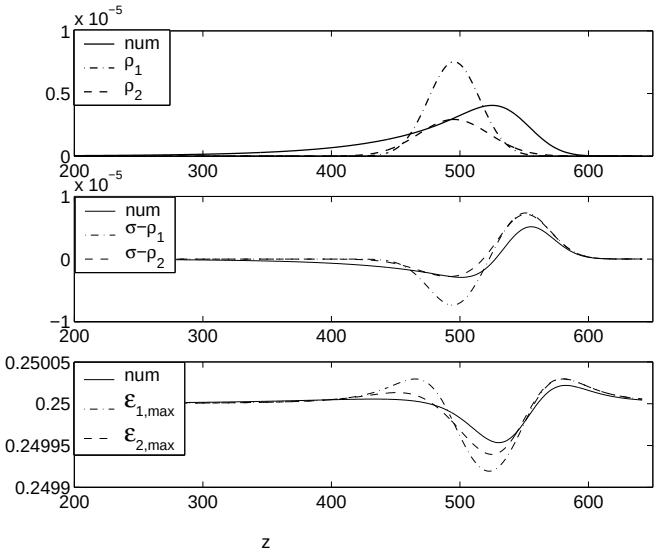

FIG. 5: The ion density (upper figure), total charge density (middle figure) and electric field (lower figure) on the axis, computed with $E_0 = 0.25$, at $\tau = 2000$. The solid lines give the numerical solution, the dash-dotted lines the solution corresponding to ρ_1 and the dotted lines to ρ_2.

V. CONCLUSIONS

In this paper, the particle distributions and associated fields of an electron avalanche in a homogeneous electric field were analyzed. During the exponential growth of the total number of electrons and ions, the electrons are described by the known Gaussian distribution, but we found that the spatial moments of the ion distribution can also be calculated. As a result, we find that the centers of mass of electron and ion distribution both travel with the electron drift velocity within the external field. For the ions this is remarkable, since they are assumed to be immobile; their center of mass motion is therefore purely due to generation of additional ions. The distance between the centers of mass is given by the ionization length $1/\alpha(E_b)$. Furthermore, the electron cloud widens homogeneously through diffusion, so its width both in the longitudinal and in the radial direction is given by $\sqrt{2D\tau}$. The ion cloud lags behind and has the somewhat smaller "delayed" radius $\sqrt{2D\tau\,[1-1/(\alpha d)]}$ in the radial direction while its extension in the longitudinal direction can be larger, in particular, for small times, as it is characterized by $\sqrt{\ell_\alpha^2 + 2D\tau\,[1-1/(\alpha d)]}$ where ℓ_α is the dimensionless version of the ionization length $1/\alpha(E_b)$.

Furthermore, we evaluate the field of the electron cloud exactly and the field of the ion cloud approximately, and derive a criterion for the avalanche to streamer transition that takes diffusion into account. It corrects Meek's criterion that stated that $\alpha d \simeq 18-21$, d being the transition travel distance and α the ionization cross section of the electrons. The transition distance strongly depends on diffusion and on the background electric field. For high

fields, the transition time saturates towards $\alpha d \simeq 15$. On the other hand, for low fields, when the processes are diffusion dominated, the avalanche lasts much longer.

The analytical models described in this paper give a useful tool to describe the negative streamer formation. Especially at relatively low, realistic, fields, the present model gives an accurate description of the avalanche to streamer transition. We stress that our criterion for the transition is based on the space charges affecting the background electric field in such a way that the linearization around it no longer holds. This corresponds to the moment that the electron cloud and its ion trail start reducing sensibly the electric field strength between them. The criteria for spark breakdown derived by Meek [15], and for positive streamer formation by Bazelyan [17] are based on the space charges screening out the field between the positively and negatively charged regions, i.e. $k = \mathcal{O}(1)$. However, their calculations are based on the linearization around the uniform background field, which obviously does not hold at these values of k. Moreover, the situation of complete screening might never be reached in the full nonlinear dynamics [21, 25, 26].

In [17] the diffusive widening of the electron was not accounted for in the derivation of the criterion. The diffusion however has considerable effects on the electron and ion distribution, and especially at low fields it can considerably delay the emergence of a streamer. Indeed, in high fields, the transition to a streamer occurs after the electron cloud has traveled a much shorter distance than expected by Bazelyan.

The nonlinear streamer propagation is the subject of other studies. In that phase the space charges and electric field strongly interact, and the analytical study of such streamers is far more difficult than the analysis of the avalanche phase [27].

Acknowledgments

C.M. acknowledges a Ph.D. grant of the Dutch NWO/FOM-programme on Computational Science.

[1] V. Mazur and P.R. Krehbiel and X. Shao, J. Geophys. Res **100**, 25731 (1995). (CRC Press, New York, 1998).
[2] E.M. Bazelyan and Yu.P. Raizer, *Lightning Physics and Lightning Protection* (Institue of Physics Publishing, Bristol, 2000)
[3] E.A. Gerken, U.S. Inan and C.P. Barrington-Leigh, Geophys. Res. Lett **27**, 2637 (2000).
[4] V.P. Pasko and H.C. Stenbaek-Nielsen, Geophys. Res. Lett. **29**, 82 (2002).
[5] N. Liu and V.P. Pasko, J. Geophys. Res **109**, A04301 (2004).
[6] F.F. Chen, Phys. Plasmas **2**,2164 (1995).
[7] B. Eliasson and U. Kogelschatz, IEEE Trans. Plasma Sci. **19**, 309 (2003).
[8] K. Shimizu, K. Kinoshita, K. Yanagihara, B.S. Rajanikanth, S. Katsura and A. Mizuno, IEEE Trans. Plasma Sci. **33**, 1373 (1997).
[9] I.V. Lisitsyn, H. Nomiyama, S. Katsuki and H. Akiyama, Rev. Sci. Instr **70**, 3457 (1999).
[10] G.J.J. Winands, K. Yan, S.A. Nair, A.J.M. Pemen and E.J.M van Heesch, Plasma Proc. and Polymers **2**, 232 (2005).
[11] M. Makarov, J. Bonnet and D. Pigache, Appl. Phys. B **66**, 417 (1998)
[12] A. Oda, H. Sugawara, Y. Sakai and H. Akashi, J. Phys. D: Appl. Phys. **33**, 1507 (2000).
[13] U. Kogelschatz, Plasma Sources Sc. and Tech. **11**, A1 (2002).
[14] A.M. van Veldhuizen, P.C.M. Kemps and W.R. Rutgers, IEEE Trans. Plasma Sci. **30**, 162 (2002).
[15] J.M. Meek, Phys. Rev. **57**, 722 (1940).
[16] Y.P. Raizer, *Gas Discharge Physics* (Springer, Berlin, 1991).
[17] E.M. Bazelyan and Yu.P. Raizer, *Spark Discharge*,
[18] L.B. Loeb, Phys. Rev. **74**, 210 (1948).
[19] U. Ebert, W. van Saarloos and C. Caroli, Phys. Rev. E, **55**, 1530 (1997).
[20] A.J. Davies, C.S. Davies and C.J. Evans, Proc. IEE **118**, 816 (1971).
[21] S.K. Dhali and P.F. Williams, J. Appl. Phys **62**, 4696 (1987).
[22] P.A. Vitello, B.M. Penetrante and J.N. Bardsley, Phys. Rev. E. **49**, 5574 (1994).
[23] A. Rocco, U. Ebert and W. Hundsdorfer, Phys. Rev. E. **66** 035102(R) (2002).
[24] C. Montijn, B. Meulenbroek, U. Ebert and W. Hundsdorfer, IEEE. Trans. Plasma Sc. **33**, 260 (2005).
[25] J. Zeleny, J. Phys. D: Appl. Phys. **13**, 444 (1942).
[26] W. Hopwood, Proc. Phys. Soc. B **62**, 657 (1949).
[27] B. Meulenbroek, A. Rocco and U. Ebert, Phys. Rev. E. **69**, 067402 (2004).